Spinally projecting noradrenergic neurons of the locus coeruleus display resistance to AAV2retro-mediated transduction

Robert P Ganley[1] (iD) **, Kira Werder[1], Hendrik Wildner[1], and Hanns Ulrich Zeilhofer[1,2,3]** (iD)

Abstract

Background: The locus coeruleus (LC) is the principal source of noradrenaline (NA) in the central nervous system. Projection neurons in the ventral portion of the LC project to the spinal cord and are considered the main source of spinal NA. To understand the precise physiology of this pathway, it is important to have tools that allow specific genetic access to these descending projections. AAV2retro serotype vectors are a potential tool to transduce these neurons via their axon terminals in the spinal cord, and thereby limit the expression of genetic material to the spinal projections from the LC. Here, we assess the suitability of AAV2retro to target these neurons and investigate strategies to increase their labelling efficiency.

Results: We show that the neurons in the LC that project to the spinal dorsal horn are largely resistant to transduction with AAV2retro serotype vectors. Compared to Cholera toxin B (CTb) tracing, AAV2retro.eGFP labelled far fewer neurons within the LC and surrounding regions, particularly within neurons that express tyrosine hydroxylase (TH), the rate-limiting enzyme for NA synthesis. We also show that the sensitivity for transduction of this projection can be increased using AAV2retro.eGFP.cre in ROSA26[tdTom] reporter mice (23% increase), with a higher proportion of the newly revealed neurons expressing TH compared to those directly labelled with AAV2retro containing an eGFP expression sequence.

Conclusion: These tracing studies identify limitations in AAV2retro-mediated retrograde transduction of a subset of projection neurons, specifically those that express NA and project to the spinal cord. This is likely to have implications for the study of NA-containing projections as well as other types of projection neuron in the central nervous system.

Background

The locus coeruleus (LC) of the dorsal pons is the main source of noradrenaline (NA) in the nervous system. With projections to most brain and spinal cord regions, it plays an important role in coordinating many global responses, such as arousal, attention, anxiety and responses to stress.[1,2] Chemogenetic activation of these neurons has demonstrated the ability of the LC to rapidly alter brain-wide connectivity and alter global behavioral responses.[3,4] Additionally, virus-based tracing of the different projections of this region have provided new insights into the anatomical organization of the LC, such as the relationship of synaptic input to the various output neurons.[5] Furthermore, viral approaches have enabled the functional characterization of specific LC output neurons to better understand the precise functional organization of this region.[6]

[1]Institute for Pharmacology and Toxicology, University of Zürich, Zürich, Switzerland
[2]Institute of Pharmaceutical Sciences, ETH Zürich, Zürich, Switzerland
[3]Neuroscience Center Zurich, Zürich, Switzerland

Corresponding Authors:
Robert P Ganley, Institute for Pharmacology and Toxicology, University of Zürich, Winterthurerstrasse 190, 8057 Zürich, Switzerland
Email: robert.ganley@pharma.uzh.ch
Hanns Ulrich Zeilhofer, Institute for Pharmacology and Toxicology, University of Zürich, Winterthurerstrasse 190, 8057 Zürich, Switzerland
Email: zeilhofer@pharma.uzh.ch

The descending projections from the LC are the main source of NA in the spinal cord. These have been shown to play important roles in pain-related behaviors, such as diffuse noxious inhibitory controls (DNIC) and tonic regulation of heat sensitivity.[7,8] Additionally, activation of this projection can reduce heat sensitivity in the Hargreaves plantar assay,[9] indicating a largely antinociceptive influence of this projection. However, the LC is also known to be involved in maintaining chronic pain states,[10] and recent studies suggest that descending NA-containing projections are involved in generating mechanical hypersensitivity via spinal astrocytes.[11] Therefore, the relationship between this structure and pain sensitivity may be more complex than previously thought.

Technologies that allow genetic access to projection neurons are highly desirable for functional and anatomical tracing studies. Recently, AAV serotypes have been developed through a process of directed evolution to efficiently transduce projection neurons via their axon terminals (AAV2retro).[12] This allows genetic access to many different types of projection neurons based on their target region and, when used in combination with cre-driver lines, neurotransmitter content, which would allow the precise functions of these projections to be determined. With respect to the LC, it would allow the functional roles of different projections to be studied through gain-of-function and loss-of-function experiments.[7,9]

In order to test whether AAV2retro vectors are suitable for tracing the descending noradrenergic pathway, we compared the labelling efficiency of LC neurons from the spinal cord using AAV2retro vectors and non-viral retrograde tracing. We find that the neurons of the LC that express Tyrosine Hydroxylase (TH) are not efficiently labelled using AAV2retro when compared to cholera toxin b (CTb) tracing. Furthermore, we show that the efficiency of labelling these noradrenergic neurons can be increased when transducing spinally projecting neurons with cre recombinase in a cre-dependent reporter mouse line. Together, we highlight limitations in the retrograde tracing capacity of AAV2retro serotype vectors for catecholaminergic pontine neurons.

Methods

Animals

Mice aged between 6–10 weeks were used for all experiments. Permission to perform these experiments was obtained from the Veterinäramt of the canton of Zürich (154/2018). The animals used were either wild-type, or ROSA26^{tdTom} transgenic animals, both of which were bred on a C57Bl/6 background

Spinal cord injections

Lumbar spinal dorsal horn injections were performed similarly to previous studies.[13] Briefly, isoflurane anaesthesia was induced at 5% in a small induction chamber, and animals were then transferred to a stereotaxic injection frame where anaesthesia was maintained at 1–3%. All surgeries were performed on a heated mat to prevent a reduction in body temperature. Animals were provided with 0.1 mg/kg buprenorphine for analgesia 20 min before starting the surgery. The back of the animal was shaved, scrubbed with betadine solution, and allowed to dry. A 2 cm incision was made on the back, and the skin was separated from the underlying tissue by blunt dissection. The T13 vertebra was identified, isolated, and clamped in position using a pair of vertebral bars that were installed on the stereotaxic frame. A small hole was drilled in the center of the vertebra on the left-hand side, and three evenly spaced injections of 300nl were given at an infusion rate of 50 nL/min at a depth of 200–300 μm from the dorsal surface of the spinal cord. Two of these injections were given above and below the clamped vertebra in the intervertebral spaces, while the third was through the drilled hole. The three injections were approximately 500 μm to the left of the central artery of the spinal cord. All injections were made through glass capillaries mounted on a 10 μl Hamilton syringe. Following each injection, the capillary was left in position for 3–5 min to allow the solution to equilibrate and to prevent backflow of the injected substance after the removal of the capillary from the tissue. After virus or CTb infusion, the back of the animal was sutured, and the wound was treated with betadine solution. Animals were recovered individually in a heated cage and were monitored post-surgery for any signs of discomfort or weight loss. Injected viruses include ssAAV-retro/2-CAG-EGFP-WPRE-SV40p(A) (UZH viral vector core facility v24-retro, titre 5.0×10^{12} viral genomes per ml (vg/ml)), ssAAV-retro/2-hSyn-EGFP-WPRE-SV40p(A) (UZH viral vector core facility v81-retro, titre 8.5×10^{12} vg/ml), and ssAAV-retro/2-CAG-EGFP-cre-WPRE-SV40p(A) (UZH viral vector core facility v25-retro, titre 5.9×10^{12} vg/ml).

Stereotaxic brain injections were performed in a similar manner to the spinal cord injections in terms of analgesia, anaesthesia, and animal care. The heads were fixed into the frame using cheek bars that were adjusted to make the skull as flat and straight as possible. Injections were made using a motorized frame controlled by a computer interface, which was also used to select the injection targets (Neurostar). The stereotaxic coordinates used were −5.4, +/−0.8, and 4 (AP, ML, and DV respectively) relative to Bregma and 500 nl of virus (ssAAV-9/2-shortCAG-EGFP-SV40p(A) UZH viral vector core facility v240-9, titre 7.0×10^{12} vg/ml) was

infused at a rate of 50 nl/min. Corrections were made for tilt and scaling using Neurostar software, which were determined by the position of 4 reference points on the skull (Bregma, Lambda, and points 2 mm to the left and right of the midline between Bregma and Lambda). Animals were perfused 14 days after virus injection.

Tissue processing and analysis

Perfusion fixation and tissue processing. Animals were perfused transcardially using a small volume of 0.1 M sodium phosphate buffer (PB) followed by 100 ml of freshly dissolved paraformaldehyde (PFA) (4% in 0.1 M PB, pH 7.4). Once fixed, the nervous tissues were dissected and post-fixed for 2 hours in 4% PFA at 4°C. After post-fixation, tissues were rinsed three times for 10 min each with 0.1 M PB and were cryoprotected in a 30% sucrose solution (dissolved in 0.1 M PB) for at least 24 hours.

Tissues were embedded in Neg50 freezing medium that was quickly frozen at −20°C. Frozen blocks were mounted on a sliding blade microtome (Hyrax KS 34, histocam AG), and sections were cut at 60 μm thickness. Sections were either stored in antifreeze medium (50 mM sodium phosphate buffer, 30% ethylene glycol, 15% glucose, and sodium azide (200 mg/L) at −20°C or were processed immediately for immunostaining.

If required, antifreeze medium was removed by rinsing sections three times for 10 min each with 0.1 M PB. Tissues were incubated for 30 min in 50% ethanol at room temperature on a shaking table. Ethanol was removed and tissue sections were rinsed three times for 10 min each in phosphate buffered saline (PBS) with extra salt added (8 g NaCl per liter PBS). Sections were then incubated at 4°C for two or three nights in primary antibodies that were diluted in PBS with extra salt, 0.3% v/v Triton-X and 10% v/v normal donkey serum. Sections were rinsed three times for 10 min each to remove unbound antibodies and bound antibodies were revealed using species specific secondary antibodies, which were all raised in donkey and conjugated to

fluorophores. All antibodies and dilutions can be found in Table 1. Incubation of the tissue in secondary antibody was overnight at 4°C. Following immunostaining, sections were again rinsed three times for 10 min each with PBS extra salt and mounted on microscope slides using Dako antifade mounting medium.

Image acquisition and analysis. Image stacks were acquired at 5 μm z-spacing using a Zeiss lsm 800 confocal microscope with Zen blue software. Confocal scans were made using 488, 561 and 640 nm lasers with the pinhole set to 1 Airy Unit for reliable optical sectioning. Care was taken to take image stacks up to a depth where there was clear fluorescent signal of all antigens. For each experiment, acquisition settings were kept constant. All images were analyzed using FIJI with the cell counter plugin. For quantification of neurons within the LC, the LC was defined as the area where there was dense immunostaining for TH.

Data collection, storage and presentation. Data obtained from the quantification of images were collected and processed in Microsoft Excel and were presented using GraphPad Prism. Representative images were produced in Affinity Photo and were annotated and arranged into figures in Affinity Designer. Raw data for these experiments are available on request and are located on the internal servers of the Institute for Pharmacology and Toxicology, University of Zürich.

Results

Neurons in the LC are rarely labelled from the spinal dorsal horn with AAV2retro

To specifically target projection neurons, AAV2retro serotype vectors have been used to transduce neurons via their axon terminals.[12–15] In order to test whether this vector serotype is suitable for transducing the various neurons that project from the brain to the spinal cord, we injected the lumbar spinal dorsal horn with

Table 1. List of antibodies used in this study.

| Antibody	Host	Supplier/Source	Cat#/RRID	Dilution
GFP	Chicken	LifeTech	A10262 / AB_2619988	1:1000
CTb	Goat	LIST biological laboratories inc.	#703 / AB_2314252	1:1000
mCherry	Rat	Molecular Probes	Cat# M11217 / AB_2536611	1:1000
TH	Sheep	Millipore	AB1542 / AB_90755	1:1000
NeuN	Guinea pig	Synaptic systems	266004 / AB_2619988	1:1000
Chicken-A488	Donkey	Jackson ImmunoResearch Laboratories	703-506-148 / AB_2340376	1:500
Goat-Cy3	Donkey	Jackson ImmunoResearch Laboratories	705-166-147 / AB_2340413	1:500
Rat-Cy3	Donkey	Jackson ImmunoResearch Laboratories	712-165-153 / AB_2340667	1:500
Guinea pig-A647	Donkey	Jackson ImmunoResearch Laboratories	706-469-148 / -	1:500
Sheep-A647	Donkey	Jackson ImmunoResearch Laboratories	713-606-147 / AB_2340752	1:500
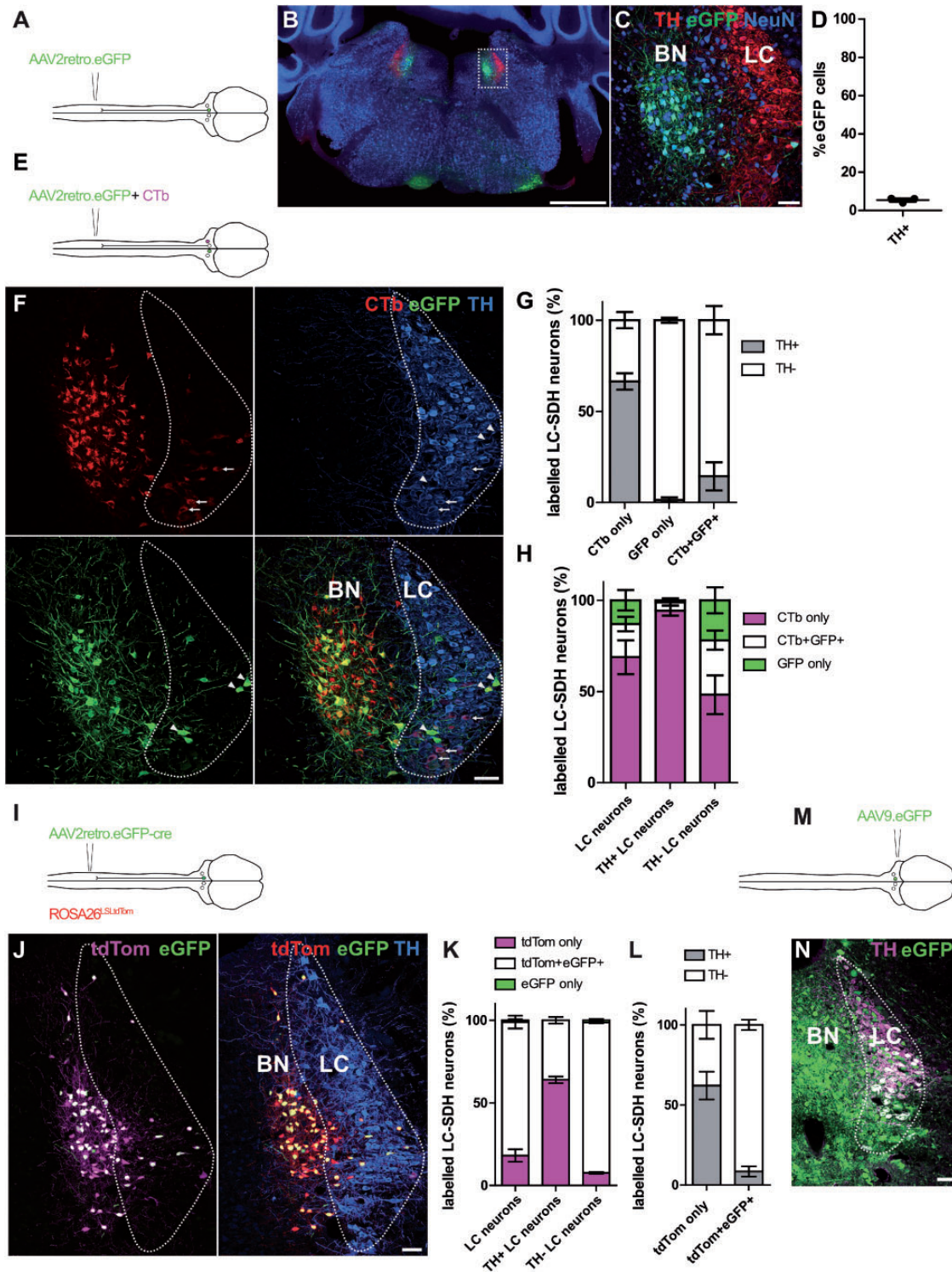
Figure 1. Labelling of spinally-projecting neurons of the locus coeruleus with AAV2retro vectors and Cholera toxin b. (a) Injection scheme for labelling spinally-projecting neurons with AAV2retro.eGFP. (b) Hindbrain section containing many eGFP-labelled neurons in the dorsal pons. Note that these eGFP neurons are mostly separate from the TH-immunoreactive locus coeruleus (LC) and are mostly present in the adjacent Barrington nucleus (BN) (scale bar = 500μm). (c) Enlargement of the boxed area in B. highlighting the area containing eGFP-labelled neurons (scale bar = 50μm). Image is a projection of two confocal scans at 5μm z-spacing. (d) Quantification of eGFP-labelled cells in the area surrounding the LC that are TH-expressing (N = 3 animals). (e) Injection scheme for AAV2retro.eGFP and CTb co-labelling experiments. (f) representative image of retrogradely labelled neurons in the LC (delimited by TH-immunoreactivity) and the Barrington nucleus (scale bar = 50μm). Arrowheads indicate retrogradely transduced neurons that are eGFP-expressing, but do not

an AAV2retro vector containing an eGFP expression cassette and analyzed the brain areas that contained eGFP-labelled neurons (Figure 1(a)). Similar to previous studies, we identified several brain areas that contained retrogradely labelled neurons.[13–15] These included neuron clusters located bilaterally in the dorsal pons (Figure 1(b)). However, we noticed that the labelled neurons surrounding the LC were rarely ever immunoreactive for tyrosine hydroxylase (TH), the rate-limiting enzyme required for NA synthesis (Figure 1(c)). Upon closer inspection, we saw a clear anatomical separation between the majority of the retrogradely traced eGFP-expressing neurons and the TH-immunoreactive region (Figure 1(b) and (c)). The area containing the majority of the eGFP+ cells was medial to the LC and was identified as the Barrington nucleus, a structure involved in micturition.[16–18] Furthermore, when the labelled neurons were examined for TH-immunoreactivity, very few eGFP+ neurons expressed detectable levels of TH, suggesting that the labeled neurons were not noradrenergic (Figure 1(d)). Therefore, we hypothesized that the neurons of the LC are resistant to AAV2retro-mediated transduction, in particular those that synthesize NA.

Comparison of CTb and AAV2retro labelled neurons

Several previous studies report retrograde tracing of noradrenergic neurons of the LC from the spinal cord using non-viral tracing methods.[19,20] To directly compare retrograde labelling with AAV2retro to a non-viral tracer, we co-injected 0.5% CTb and the AAV2retro. GFP used in the previous experiment (Figure 1(e)). In agreement with previous studies, CTb-labelled neurons were found within the LC, and many of those were immunoreactive for TH (Figure 1(f)). In addition, we also detected many CTb+ neurons within the adjacent Barrington nucleus.

We then compared the eGFP- with the CTb-traced neurons present within the LC, which we defined as the area of dense TH staining in the dorsal pons. In general, more CTb+ neurons (337) were labelled in the LC compared to the GFP+ neurons (104) (Figure 1(f) and Table 2). Most of the neurons that were labelled with eGFP also contained CTb (62/104), although many cells expressed eGFP only (42/104) (Figure 1(f) and Table 2). When we examined the traced neurons for TH content, we found that a much higher proportion of CTb-only neurons expressed detectable TH (66.3%) compared to eGFP-only (1.4%), and neurons that expressed both CTb and eGFP (14.4%)(Figure 1(g)). Furthermore, when we looked at the total population of retrogradely traced neurons that did not express TH, neurons that contained eGFP were much more highly represented (21.9% and 48.2% of eGFP-only and CTB+eGFP+ neurons respectively) (Figure 1(h)). Together, this suggests that within the LC, spinally-projecting TH+ neurons are more resistant to

Table 2. Cell counts for LC neurons retrogradely labelled from the spinal dorsal horn with AAV2retro.eGFP and Ctb.

Injected material (number of animals)	Subset	eGFP only	Ctb only	eGFP+Ctb+	%eGFP only	%Ctb only	%eGFP+Ctb+
AAV2retro.CAG.eGFP + 0.5% Ctb (n = 4)	All LC neurons	42 (4–18)	275 (29–124)	62 (11–21)	13.0 (3.6–28.1)	68.8 (45.3–88.6)	18.2 (7.9–26.6)
	TH+	1 (0–1)	185 (20–90)	8 (0–4)	1.1 (0–4.3)	94.3 (87–100)	4.6 (0–8.7)
	TH–	41 (4–17)	90 (9–34)	54 (7–19)	21.9 (10.9–41.5)	48.2 (22–73.9)	29.9 (15.2–38.2)
AAV2retro.hSyn.eGFP + 0.5% Ctb (n = 4)	All LC neurons	40 (5–16)	145 (24–49)	65 (7–25)	15.7 (10.4–18.4)	58.7 (54.4–63.2)	25.6 (18.4–33.3)
	TH+	2 (0–1)	133 (22–43)	3 (0–3)	1.5 (0–4.3)	96.4 (91.3–100)	2.2 (0–6.5)
	TH–	38 (5–16)	12 (1–6)	62 (7–25)	33.9 (22–40)	10.7 (4.5–13.3)	55.4 (46.7–72.7)

Numbers indicate the total counted neurons per group, with the range of neurons counted per animal in parentheses. Percentages are an average value, with the range included in parentheses.

Figure 1. Continued
contain TH immunoreactivity. Arrows highlight TH-expressing neurons that were retrogradely labelled with CTb only. Image is a projection of two confocal scans at 5μm z-spacing. (g) Quantification of CTb- and eGFP-labelled neurons that are present in the LC. The proportion of traced neurons that express TH are quantified for each group (N = 4 animals). (h) Data from G. showing the proportion of each retrograde marker present in all LC neurons, TH-expressing LC neurons, and neurons that do not contain detectable TH levels. (i) Injection scheme to increase AAV2retro-mediated labelling efficiency by transduction with cre rather than eGFP alone. (j) Representative image of the LC of ROSA26[LSLtdTOM] animals that received a spinal dorsal horn injection with AAV2retro.eGFP-cre (scale bar = 50μm). Image is a projection of two confocal scans at 5μm z-spacing. (k) Quantification of the proportion of LC neurons that express tdTOM-only, eGFP and tdTOM, and eGFP-only (N = 3 animals). (l) The same data as (k) but displayed as a proportion of tdTOM-only and eGFP and tdTOM-expressing neurons that are either TH+ or TH-. (m) Injection scheme for the direct labelling of LC neurons by stereotaxic brain injection. (n) Representative image of the LC containing many eGFP-labelled neurons that are also TH-expressing. Image is a single optical section (scale bar = 50μm).

AAV2retro transduction than surrounding TH– neurons.

Recent studies have used a similar strategy to manipulate spinally-projecting noradrenergic neurons using AAV2retro serotype vectors, and reported efficient labelling of these neurons from the spinal cord.[11,21,22] One possible explanation for differences between these findings and the present study could be the promoter choice and subsequent expression of genetic material in noradrenergic neurons. To explore this possibility, we repeated our tracing studies with CTb and AAV2retro vectors containing a hSyn promoter instead of the CAG promoter used in the previous experiment. We found broadly the same pattern of labelling, with eGFP-labelled cells being underrepresented within TH-expressing LC neurons (eGFP-only = 1.5%, eGFP+CTb+ = 2.2%, CTb-only = 96.4%, Table 2). In contrast, virtually all eGFP-only neurons were devoid of detectable TH (38/40). Taken together this indicates that the lack of eGFP labelling is due to a resistance of TH-expressing neurons to AAV2retro-mediated transduction, rather than low transcriptional activity from the promoter in these cells (summary of data in Table 2).

Enhanced tracing efficiency with retrograde transduction of cre versus eGFP

The lack of TH+ LC neurons traced from the spinal cord could either be due to the complete resistance of these neurons to AAV2retro transduction, or due to a low number of viral particles entering these neurons, resulting in a low to undetectable expression of eGFP. To test whether we could increase AAV2retro-mediated labelling of TH+ neurons with a more sensitive method, we injected ROSA26^{LSLtdTomato} reporter mice with AAV2retro.eGFP.cre, which contains an eGFP-cre fusion protein expression sequence. Using a cre recombinase and the cre-dependent tdTomato reporter allele should be a more sensitive tracing method, which can be compared to the direct labelling with eGFP (Figure 1(i)).

Within the LC, we observed many tdTom-expressing neurons whose nuclei were labelled with eGFP (80.8% of traced LC neurons) (Figure 1(j)). This pattern of eGFP expression is consistent with the expression of cre being largely confined to the neuronal nuclei.[23,24]

In addition, we observed many tdTom-expressing neurons that did not contain detectable eGFP expression (18.1% of labelled LC neurons), which, we believe, is due to low to undetectable cre-eGFP expression (Figure 1(j)). We almost never observed neurons expressing eGFP without tdTom (2/205 labelled LC neurons) (Table 3 and Figure 1(k)). In this analysis we considered tdTom-only neurons as "newly revealed" due to increased labelling sensitivity, whereas tdTom+eGFP+ neurons were considered to be cells that could be traced and detected directly with fluorophore alone.

We found that the increase in labelling sensitivity was modest, with an increased labelling of 23% (Figure 1(j)). Within the "newly revealed" neurons (tdTom-only), we found that a higher proportion contained detectable TH immunoreactivity (TH+ 25/38, TH– 13/38). Within the tdTom-only group, this corresponded to 65.8% and 34.2% of TH+ and TH– LC neurons, respectively (Figure 1(l)). In contrast a higher proportion of "directly labelled" eGFP+tdTom+ cells did not contain TH (TH+ = 8.5%, TH– = 91.5%). Therefore, we conclude that the possible increase in labelling efficiency that could be achieved by retrograde transport of DNA recombinases using AAV2retro is minor, although it preferentially increases labelling of TH+ neurons.

An alternative explanation for the limited TH staining in neurons labelled with AAV2retro is due to a downregulation of the enzyme following AAV transduction and a subsequent loss of immunoreactivity. To test this directly, we injected AAV9.eGFP bilaterally into the LC of three animals (Figure 1(m)). In all animals we could identify many TH-expressing neurons within the injection site that were labelled with eGFP (Figure 1(n)). Taken together, this suggests that the lack of TH expression in AAV2retro labelled neurons is most likely due to a resistance of these neurons to retrograde transduction, rather than a loss of TH immunoreactivity.

Discussion

Main findings

The main findings of the current study are: (1) that most TH-containing LC neurons that project to the spinal cord display resistance to AAV2retro-mediated

Table 3. Increased labelling of LC neurons with AAV2retro.cre.eGFP and ROSA26^{LSLtdTom} reporter mice.

Subset of LC neurons	eGFP only	tdTom only	eGFP+tdTom+	%eGFP only	%tdTom only	%eGFP+tdTom+
All neurons	2 (0–1)	38 (7–19)	165 (44–67)	1.1 (0–1.9)	18.1 (13.5–25.7)	80.8 (73–84.8)
TH+	0 (0–0)	25 (4–15)	14 (2–8)	0 (0–0)	64.0 (60–66.7)	35.9 (33.3–40)
TH–	2 (0–1)	13 (3–6)	151 (42–63)	1.3 (0–2.2)	7.7 (6.5–8.7)	91.0 (90.2–91.3)

Numbers indicate a total count from all animals, whereas percentages are an average value. The range of cells counted and percentage per animal are given in parentheses (n = 3 animals).

retrograde transduction through their spinal terminals; (2) that differences in retrograde labelling efficiency are observed between AAV2retro and CTb labelling; and (3) that retrograde AAV2retro-mediated transduction with cre-recombinase and a cre-dependent reporter line is a more sensitive labelling method than transduction with fluorescent proteins alone, but only increase the total labelling of TH-containing LC projections slightly.

Resistance of TH+ neurons to AAV2retro transduction

Since the development of the AAV2retro serotype,[12] there have been reports that certain populations of projection neuron are resistant to AAV2retro-mediated transduction. Specifically, lower labelling efficiency is observed in serotonergic neurons of the nucleus raphe magnus that project to the spinal cord, as well as dopaminergic neurons projecting from the substantia nigra pars compacta to the dorsomedial striatum.[12,15] In the present study, we find that the noradrenergic neurons within the LC are also resistant to transduction with AAV2retro through their spinal axon terminals. We also show that these neurons do not show resistance to AAV vectors that are directly injected into the LC in agreement with previous studies.[4]

The AAV2retro was developed using a process of directed evolution, by injecting known projection targets with AAVs, harvesting the tissue where the projection neurons originate, and amplifying the AAV capsid proteins present in this tissue using an error prone polymerase.[12] This process was repeated to obtain an AAV with increased retrograde labelling efficiency. Notably, the well-characterized projections that were used for this directed evolution were excitatory neurons projecting from the hindbrain to the cerebellar cortex, or inhibitory striatal neurons that projected to the substantia nigra pars reticulata, which do not communicate using catecholamine neurotransmitters.[12] Consequently, the increased efficiency obtained through this strategy may be less well suited for projection neurons that operate through catecholaminergic neurotransmission.

Other viral strategies have been used to selectively activate noradrenergic LC to spinal cord projections, such as using canine adenoviruses.[6,7,9] This strategy has enabled the selective activation of spinally-projecting NA neurons in the LC of the rat by expression of pharmacological actuators under the control of the synthetic promoter PRSx8 (9). Therefore, it seems likely that AAV2retro vectors are not ideal for functional studies of descending noradrenergic circuits, whereas alternative retrograde labelling strategies may be better suited.

Differences in labelling between CTb and AAV2retro

In addition to the low transduction efficiency of TH-containing LC neurons, many labelled neurons in this region were transduced with AAV2retro but did not contain detectable CTb labelling. This raises the possibility that AAV2retro-transduction may be better placed to trace some projections than non-viral methods. This is likely due to increased sensitivity of the labelling strategy when compared to other tracing techniques. Notably the group that contained most GFP-only neurons was LC neurons that did not contain TH (Figure 1(h)), consistent with the idea that AAV2retro preferentially transduces neurons that use fast amino acid transmitters. The identification of non-noradrenergic neurons of the LC that project to the spinal cord raises the possibility of functional heterogeneity within the descending pontospinal pathway.

Sensitivity of AAV2retro-mediated retrograde labelling with cre versus eGFP

Recently, similar strategies have been used to functionally manipulate descending LC neurons by injecting AAV2retro serotype vectors into the spinal cord.[11,21,22] In one study, AAV2retro.ESYN.cre was used to transduce projections to the spinal cord with cre, and bilateral injections into the LC with an AAV containing a cre-dependent hM3Dq were used to activate NA-containing LC neurons that project to the spinal cord.[11] This intersectional approach may be a more sensitive strategy, leading to a more efficient capture of the NA-containing neurons. Accurate injection of small volumes of cre-dependent effectors into the LC may also avoid labelling the adjacent Barrington nucleus. However, it is likely that these approaches will mostly affect LC projection neurons that do not express TH or NA, since these are more commonly labelled with the AAV2retro from the spinal cord. One difference between our results and those of Kohro et al.[11] is the promoter choice, which were CAG and hSyn promoters and ESYN respectively. We obtained similar results using CAG and hSyn promoters, suggesting that these promoters are similarly active in noradrenergic neurons. Although promoter choice could influence transcription of the eGFP gene, this is unlikely to be a limiting factor in our experiments since injection of AAVs containing the CAG promoter directly into the LC were able to label many TH-containing neurons with eGFP, indicating that this promoter is transcriptionally active in these neurons. Together this indicates that the likely explanation for the lack of labelling in noradrenergic neurons is the entry of AAV2retro into the axon terminals of these cells, or the lack of retrograde transport of the genetic material.

Interestingly, the proportion of tdTom-only TH+ neurons labelled using AAV2r.eGFP.cre and cre-dependent reporter mice was similar to that of the CTb labelling (CTb-only = 67.3% TH+, tdTom-only = 65.8% TH+). Therefore, it is possible that an intersectional strategy could increase the labelling sensitivity of TH+ neurons with AAV2retro vectors, especially when combined with cre driver lines.[21] However, this likely increase is rather modest, since a total increase of 23% in traced cells was seen with cre transduction, relative to the eGFP labelling. Compared to CTb labelling, AAV2retro transduction is far less efficient at labelling noradrenergic neurons (TH+ neurons retrogradely labelled from the spinal cord = 95.4% CTb-containing, vs 4.6% GFP-containing), and a small increase in this AAV2retro-mediated labelling would not result in a comparable labelling efficiency to CTb labelling. Nevertheless, this low efficiency approach is perhaps sufficient in certain experimental settings to induce measurable changes.[21]

In summary, we identify limitations of using AAV2retro vectors to retrogradely transduce noradrenergic neurons via their axon terminals. This finding is consistent with reports that the AAV2retro serotype does not have equal tropism for all projection neurons.[12,25] It is likely that other types of projection neuron will display similar resistance to AAV2retro-mediated transduction and highlights the need for alternative non-toxic retrograde tracing technologies.

Author Contributions

RPG, HW and HUZ designed the study. RPG and KW performed the experiments and analyzed the data. RPG wrote the manuscript with input from all the authors.

Declaration of conflicting interests

The author(s) declared no potential conflicts of interest with respect to the research, authorship, and/or publication of this article.

ORCID iDs

Robert P Ganley https://orcid.org/0000-0001-8502-9870
Hanns Ulrich Zeilhofer https://orcid.org/0000-0001-6954-4629

References

1. Khroud NK, Reddy V, Saadabadi A. *Neuroanatomy, locus ceruleus*. Treasure Island, FL: StatPearls Publishing, 2020.
2. Morris LS, McCall JG, Charney DS, Murrough JW. The role of the locus coeruleus in the generation of pathological anxiety. *Brain Neurosci Adv* 2020; 4: 2398212820930321.
3. Floriou-Servou A, von Ziegler L, Waag R, Schläppi C, Germain PL, Bohacek J. The acute stress response in the multiomic era. *Biol Psychiatry* Epub ahead of print 17 March 2021. DOI: 10.1016/j.biopsych.2020.12.031.
4. Zerbi V, Floriou-Servou A, Markicevic M, Vermeiren Y, Sturman O, Privitera M, von Ziegler L, Ferrari KD, Weber B, De Deyn PP, Wenderoth N, Bohacek J. Rapid reconfiguration of the functional connectome after chemogenetic locus coeruleus activation. *Neuron* 2019; 103: 702–718.e5.
5. Schwarz LA, Miyamichi K, Gao XJ, Beier KT, Weissbourd B, DeLoach KE, Ren J, Ibanes S, Malenka RC, Kremer EJ, Luo L. Viral-genetic tracing of the input-output organization of a central noradrenaline circuit. *Nature* 2015; 524: 88–92.
6. Borodovitsyna O, Duffy BC, Pickering AE, Chandler DJ. Anatomically and functionally distinct locus coeruleus efferents mediate opposing effects on anxiety-like behavior. *Neurobiol Stress* 2020; 13: 100284.
7. Howorth PW, Thornton SR, O'Brien V, Smith WD, Nikiforova N, Teschemacher AG, Pickering AE. Retrograde viral vector-mediated inhibition of pontospinal noradrenergic neurons causes hyperalgesia in rats. *J Neurosci* 2009; 29: 12855–12864.
8. Bannister K, Patel R, Goncalves L, Townson L, Dickenson AH. Diffuse noxious inhibitory controls and nerve injury: restoring an imbalance between descending monoamine inhibitions and facilitations. *Pain* 2015; 156: 1803–1811.
9. Hirschberg S, Li Y, Randall A, Kremer EJ, Pickering AE. Functional dichotomy in spinal- vs prefrontal-projecting locus coeruleus modules splits descending noradrenergic analgesia from ascending aversion and anxiety in rats. *Elife* 2017; 6: 10–14.
10. Taylor BK, Westlund KN. The noradrenergic locus coeruleus as a chronic pain generator. *J Neurosci Res* 2017; 95: 1336–1346.
11. Kohro Y, Matsuda T, Yoshihara K, Kohno K, Koga K, Katsuragi R, Oka T, Tashima R, Muneta S, Yamane T, Okada S, Momokino K, Furusho A, Hamase K, Oti T, Sakamoto H, Hayashida K, Kobayashi R, Horii T, Hatada I, Tozaki-Saitoh H, Mikoshiba K, Taylor V, Inoue K, Tsuda M. Spinal astrocytes in superficial laminae gate brainstem descending control of mechanosensory hypersensitivity. *Nat Neurosci* 2020; 23: 1376–1387.
12. Tervo DGR, Hwang B-Y, Viswanathan S, Gaj T, Lavzin M, Ritola KD, Lindo S, Michael S, Kuleshova E, Ojala D, Huang C-C, Gerfen CR, Schiller J, Dudman JT, Hantman

AW, Looger LL, Schaffer DV, Karpova AY. A designer AAV variant permits efficient retrograde access to projection neurons. *Neuron* 2016; 92: 372–382.

13. Haenraets K, Albisetti GW, Foster E, Wildner H. Adeno-associated virus-mediated transgene expression in genetically defined neurons of the spinal cord. *J Vis Exp* 2018; 135: 57382.

14. Frezel N, Platonova E, Voigt FF, Mateos JM, Kastli R, Ziegler U, Karayannis T, Helmchen F, Wildner H, Zeilhofer HU. In-depth characterization of layer 5 output neurons of the primary somatosensory cortex innervating the mouse dorsal spinal cord. *Cerebral Cortex Commun* 2020; 1; tgaa052.

15. Wang Z, Maunze B, Wang Y, Tsoulfas P, Blackmore MG. Global connectivity and function of descending spinal input revealed by 3D microscopy and retrograde transduction. *J Neurosci* 2018; 38: 10566–10581.

16. Ito H, Sales AC, Fry CH, Kanai AJ, Drake MJ, Pickering AE. Probabilistic, spinally-gated control of bladder pressure and autonomous micturition by barrington's nucleus CRH neurons. *Elife* 2020; 9: 4–30.

17. Yao J, Zhang Q, Liao X, Li Q, Liang S, Li X, Zhang Y, Li X, Wang H, Qin H, Wang M, Li J, Zhang J, He W, Zhang W, Li T, Xu F, Gong H, Jia H, Xu X, Yan J, Chen X. A corticopontine circuit for initiation of urination. *Nat Neurosci* 2018; 21: 1541–1550.

18. Rahman M, Siddik AB. *Neuroanatomy, pontine micturition center*. Treasure Island, FL: StatPearls Publishing, 2021.

19. Kwiat GC, Basbaum AI. The origin of brainstem noradrenergic and serotonergic projections to the spinal cord dorsal horn in the rat. *Somatosens Mot Res* 1992; 9: 157–173.

20. Sluka KA, Westlund KN. Spinal projections of the locus coeruleus and the nucleus subcoeruleus in the Harlan and the Sasco Sprague-Dawley rat. *Brain Res* 1992; 579: 67–73.

21. Koga K, Shiraishi Y, Yamagata R, Tozaki-Saitoh H, Shiratori-Hayashi M, Tsuda M. Intrinsic braking role of descending locus coeruleus noradrenergic neurons in acute and chronic itch in mice. *Mol Brain* 2020; 13: 144.

22. Kawanabe R, Yoshihara K, Hatada I, Tsuda M. Activation of spinal dorsal horn astrocytes by noxious stimuli involves descending noradrenergic signaling. *Mol Brain* 2021; 14: 79.

23. Foster E, Wildner H, Tudeau L, Haueter S, Ralvenius WT, Jegen M, Johannssen H, Hösli L, Haenraets K, Ghanem A, Conzelmann K-K, Bösl M, Zeilhofer HU. Targeted ablation, silencing, and activation establish glycinergic dorsal horn neurons as key components of a spinal gate for pain and itch. *Neuron* 2015; 85: 1289–1304.

24. Lemberger T, Parlato R, Dassesse D, Westphal M, Casanova E, Turiault M, Tronche F, Schiffmann SN, Schütz G. Expression of Cre recombinase in dopaminoceptive neurons. *BMC Neurosci* 2007; 8: 4.

25. Wang D, Tawfik VL, Corder G, Low SA, François A, Basbaum AI, Scherrer G. Functional divergence of delta and mu opioid receptor organization in CNS pain circuits. *Neuron* 2018; 98: 90–108.e5.